

# The yield strength and dynamic behaviour of dislocations in MgO crystals at high temperatures

FUMIO SATO\*, KOJI SUMINO

*The Research Institute for Iron, Steel and Other Metals, Tohoku University, Sendai, Japan*

The mechanical behaviour and mobility of dislocations in MgO crystals in the temperature range 20 to 800° C are shown to be dependent on the concentration and the valence state of impurities. Impurities of trivalent state are found to interrupt the motion of screw dislocations and lead to an increase of the yield strength throughout the temperature range investigated. Impurities of divalent state, of which Ca<sup>2+</sup> ions are the most prevalent, are shown to retard the motion of edge dislocations by forming an atmosphere at elevated temperatures and are responsible for a peak of the yield stress appearing around 700° C.

## 1. Introduction

It has been reported that the strength of MgO crystals is influenced markedly by impurities existing in the trivalent state such as Fe<sup>3+</sup>, Cr<sup>3+</sup>, Al<sup>3+</sup>. A rapid increase in the yield stress with a decrease in temperature has been observed in the temperature region below 300° C and has often been interpreted in terms of the thermally activated motion of dislocations overcoming obstacles associated with trivalent impurities [1-6].

Measurements of the velocity of dislocations in MgO have also been conducted in the low-temperature region by means of the etching method [7-10]. It has been shown that screw dislocations move slower than edge dislocations and the mobilities of both edge and screw dislocations increase with increase in temperature up to 150° C. The mobilities of both types of dislocation have been found to decrease by the addition of iron as an impurity which is thought to exist in the trivalent state.

*In situ* observations of the motion of dislocations at room temperature have been done with the use of HVEM [11, 12]. Screw dislocations have been observed to move slower than edge dislocations and their motion has seemed to be controlled by local obstacles. Both impurities and jogs seemed to act as such local obstacles.

On the other hand, it has been reported that MgO crystals show a peculiar behaviour in the temperature dependence of the yield stress in a relatively high temperature region which is similar to that observed in fcc alloy crystals [2,3,13]; namely, the appearance of the plateau and the following maximum in the yield stress. There have been many disputes on the origin of such peculiar behaviour especially in alloys. The most important point of the disputes lies in whether such behaviour is associated with the mobility of individual dislocations or with the development of an impurity atmosphere around dislocations. However, measurements of the mobility of dislocations in such a temperature region have never been conducted.

In this paper, the temperature dependence of the mechanical behaviour of MgO crystals with a controlled state of impurities is measured in a relatively high temperature region. With the crystals in the same state, the dynamical characteristics of dislocations are also observed by means of both the etch pit method and *in situ* observations by HVEM in the same temperature region. On the basis of such observations, a possible origin for the plateau and the maximum in the yield stress are discussed.

\* Present address: NHK Broadcasting Science Research Laboratories, Setagaya-ku, Tokyo.

TABLE I Impurity contents (wt %) of specimens

Impurity	Fe	Al	Cr	Ca	Cu	Si, Ti, Mn, Zn, Ni
Crystal I	0.003	0.003	< 0.001	0.004	0.002	< 0.001
Crystal II	0.005	0.006	0.013	0.030	< 0.001	< 0.001

## 2. Specimen preparation

Two types of MgO crystals,  $10 \times 10 \times 20 \text{ mm}^3$  in size, having different amounts of impurities were obtained from Tateho Chemical Industry. They were distinguished as crystals I and II, respectively. Impurity contents of these crystals are given in Table I. The main impurities were Fe, Al, Cr, and Ca. Crystal II contained Fe and Al in amounts twice as high and Cr and Ca to within an order of magnitude as high as those of crystal I.

Specimens for compressive deformation and those for measurements of dislocation mobility were cleaved from these crystals. The dimensions of the specimens were approximately  $2.5 \times 2.5 \times 8.0 \text{ mm}^3$  for the former and  $1.0 \times 2.0 \times 20 \text{ mm}^3$  for the latter. In order to standardize the valence state of impurities Fe, Al and Cr, all specimens were subjected to heat-treatment: annealing at  $2000^\circ \text{C}$  for 2 h in a graphite crucible in an argon gas atmosphere. This treatment was thought to reduce a considerable amount of the above impurities to the divalent state [1]. Specimens cleaved from crystal I and subjected to this heat-treatment are denoted as specimen A and those from crystal II subjected to the same treatment as specimen B. Specimen C was prepared from specimen B by sub-

jecting it to a further annealing at  $1300^\circ \text{C}$  for 24 h in air. By this treatment, impurities which had been reduced to the divalent state by the former treatment, were thought to be oxydized into the trivalent state [13]. In all cases, specimens were cooled rapidly after heat-treatment in order to avoid precipitation which was thought to take place in a temperature range below  $1000^\circ \text{C}$ . The content of trivalent impurities is thought to be in order A, B, C, specimen A containing the least.

The specimen surface ( $100 \mu\text{m}$  thick) was removed after heat-treatment by immersing into boiling phosphoric acid. The average size of subgrains in specimens was 1 mm and the density of dislocations inside subgrains was approximately  $10^3 \text{ cm}^{-2}$  after the above heat-treatment according to etch-pit counting. The dislocation etchant consisted of  $\text{H}_2\text{O}:\text{H}_2\text{SO}_4$ :saturated aqueous-solution of  $\text{NH}_4\text{Cl} = 1:1:5$ .

## 3. Deformation experiments

Specimens were deformed by compression along  $[010]$  with the use of an Instron-type machine equipped with a high-temperature compression jig, in a vacuum of about  $10^{-5}$  Torr. Yield-point phenomena were not observed on stress-strain

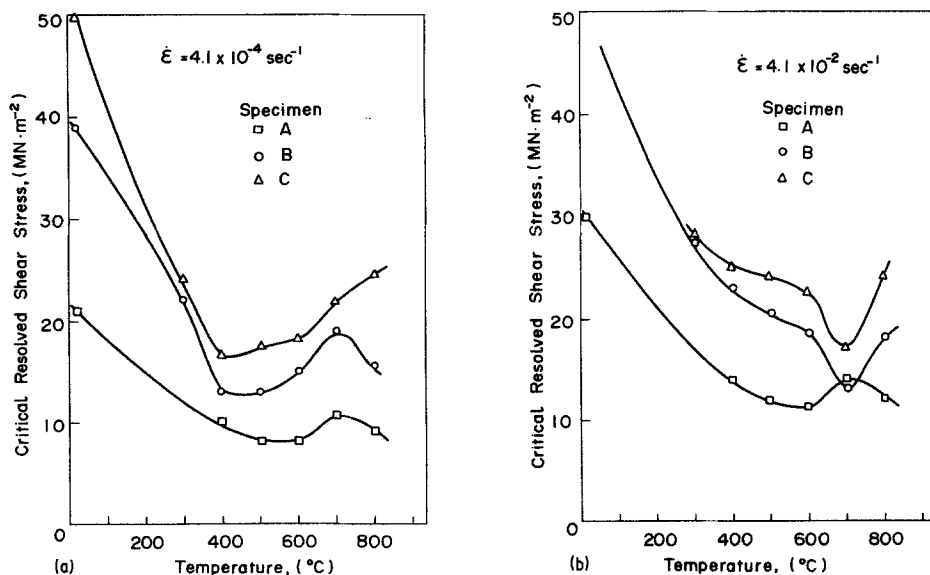


Figure 1 The critical resolved shear stress (CRSS) of various types of MgO crystals plotted against temperature for shear strain rates (a)  $\dot{\epsilon} = 4.1 \times 10^{-4} \text{ sec}^{-1}$ , and (b)  $\dot{\epsilon} = 4.1 \times 10^{-2} \text{ sec}^{-1}$ .

curves for all deformation conditions adopted. Thus, the critical resolved shear stress was defined by the resolved shear stress at which the deviation from the linear part in the initial rise of the stress-strain curve was first detected. No appreciable serration in the stress-strain behaviour was observed in specimens subjected to the heat-treatments described in Section 2 for any deformation condition adopted in the present investigation.

Fig. 1a and b show the critical resolved shear stress (CRSS) of specimens A, B and C plotted against temperature for the deformation at shear strain rates  $\dot{\epsilon} = 4.1 \times 10^{-4}$  and  $\dot{\epsilon} = 4.1 \times 10^{-2}$  sec<sup>-1</sup>, respectively. The general feature in the dependence of CRSS on the temperature seen in Fig. 1 is similar to that observed in fcc alloy crystals. The magnitude of CRSS is the lowest in specimen A and the highest in specimen C throughout the temperature range 20 to 800° C for the deformation at lower strain rates. The same holds also for the deformation at higher strain rates except at temperatures around 700° C. It may be concluded that the increase in the total amount of impurities generally results in the increase in CRSS, an anomaly appearing in a temperature range around 700° C in the case of the deformation at higher strain rates. It is also concluded that the increase in the concentration of trivalent impurities leads to the increase in CRSS throughout the temperature range investigated for any strain rates.

Clear plateaux appear for the deformation at lower strain rates in all specimens. The temperature where the plateau begins depends on the purity of the specimens. It begins at about 500° C in specimen A and at about 400° C in specimens B and C for  $\dot{\epsilon} = 4.1 \times 10^{-4}$  sec<sup>-1</sup>. Thus, this temperature seems to depend on the total amount of impurities but not on the relative concentration of trivalent and divalent impurities. The appearance of the plateau is influenced by the strain rate. No clear plateau appears in deformation at high strain rate as seen in Fig. 1b.

The peak of CRSS is observed at 700° C in specimens A and B for  $\dot{\epsilon} = 4.1 \times 10^{-4}$  sec<sup>-1</sup>; it seems to appear at a higher temperature in specimen C. For higher strain rates the peak in specimen A remains at the same temperature, but that in specimen B shifts to a higher temperature. A remarkable minimum in CRSS is observed at 700° C in specimens B and C in the deformation at  $\dot{\epsilon} = 4.1 \times 10^{-2}$  sec<sup>-1</sup>. Thus, it may be concluded

that the cause of the peak at 700° C for  $\dot{\epsilon} = 4.1 \times 10^{-4}$  sec<sup>-1</sup> is different between specimens A and B.

Throughout the temperature range from 20 to 800° C the magnitude of CRSS in specimen A is higher for higher strain rates. The same also holds in specimens B and C, except at temperatures close to 700° C. They show anomalous strain-rate dependence of CRSS at 700° C.

Peaks of CRSS appearing at relatively high temperatures in some kinds of ordered alloys and intermetallic compounds are often attributed to the activation of dislocations on slip planes other than those operating in the lower temperature range [14–16]. To see the possibility of the operation of non- $\{110\}$  slip planes at elevated temperatures, the distribution of slip bands developed on the surface of deformed specimens was observed as a function of temperature with the use of dislocation etch pits. It has been confirmed that only  $\{110\}$  slip planes operate throughout the temperature range investigated.

Stress-strain curves of specimens A, B and C are all found to consist of two deformation stages having different work-hardening rates; stages I and II similar to those in fcc metal crystals. In any kind of specimen deformed at lower strain rate,  $\dot{\epsilon} = 4.1 \times 10^{-4}$  sec<sup>-1</sup>, the work-hardening rates in both stages I and II are observed to increase rapidly with increase in temperature in the temperature range above 600° C.

Fig. 2 shows a stress-strain curve of specimen B deformed at  $\dot{\epsilon} = 4.1 \times 10^{-4}$  sec<sup>-1</sup>, the temperature being cycled between 400 and 700° C. The deformation is interrupted while the temperature is changed from 400 to 700° C or from 700 to 400° C. As has been seen in Fig. 1a, CRSS of annealed specimen B shows a minimum and a maximum at these two temperatures for  $\dot{\epsilon} = 4.1 \times 10^{-4}$  sec<sup>-1</sup>. As seen in the figure, the flow stress at 700° C seems not to be influenced by the preceding deformation at 400° C, while that at 400° C is markedly influenced by the preceding deformation at 700° C. The specimen which has undergone deformation at 700° C shows a higher magnitude of CRSS in subsequent deformation at 400° C compared with those of annealed specimens deformed at either 400 or 700° C. Another important behaviour of such a specimen is a marked decrease in the flow stress with strain after yielding.

Fig. 3 shows a stress-strain curve of specimen

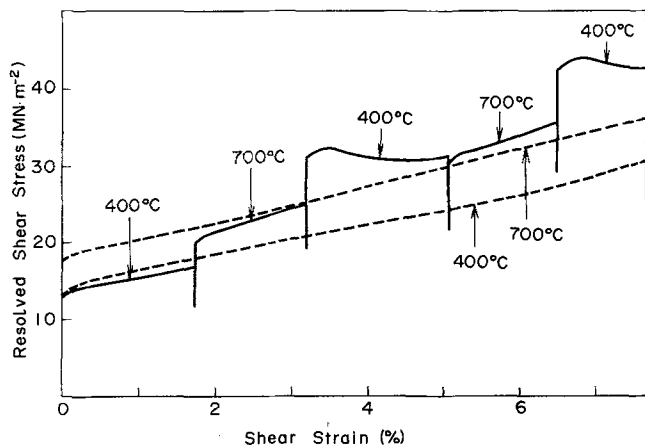


Figure 2 The effect of the temperature cycling between 400 and 700°C during the deformation of specimen B at  $\dot{\epsilon} = 4.1 \times 10^{-4} \text{ sec}^{-1}$  on the stress-strain behaviour. The broken curves are the stress-strain curves of specimens B deformed at the same strain rate when the temperatures are 400 and 700°C throughout a whole deformation state.

B which is deformed first at 700°C and  $\dot{\epsilon} = 4.1 \times 10^{-2} \text{ sec}^{-1}$  and subsequently at 400°C and  $\dot{\epsilon} = 4.1 \times 10^{-4} \text{ sec}^{-1}$ . The magnitude of CRSS of annealed specimen B at these two deformation conditions are almost the same. As in the case of Fig. 2, the flow stress in the deformation at 400°C and  $\dot{\epsilon} = 4.1 \times 10^{-4} \text{ sec}^{-1}$  after preceding deformation at 700°C and  $\dot{\epsilon} = 4.1 \times 10^{-2} \text{ sec}^{-1}$ , is higher than that of annealed specimens deformed even at 700°C and  $\dot{\epsilon} = 4.2 \times 10^{-4} \text{ sec}^{-1}$ .

The above results seem to show that the flow stress of a specimen having an internal structure developed during deformation at 700°C is higher at 400°C than at 700°C. Thus, the peak of CRSS at 700°C seen in Fig. 1a is thought to be associated with the development of some special internal structure during the deformation at that temperature and not with the temperature dependence of the mobility of individual dislocations.

#### 4. Measurements of dislocation velocity

Half loops of fresh dislocations on {110} slip planes were introduced by rolling a steel ball on

the (100) top surface of specimens at room temperature. By removing the surface regions by chemical polishing, isolated loops of fresh dislocations were obtained.

Specimens were stressed by means of bending with the use of a stress pulser. Since the shape of the stress pulse was not strictly rectangular, the magnitude of the applied stress was taken as 0.9 times the maximum of the applied stress, and the duration of stressing as the period between two time-points where the magnitude of the applied stress was equal to the above value. This procedure is justified because of the large values of the stress exponent of the dislocation velocity. The apparatus for stressing specimens at elevated temperatures is shown schematically in Fig. 4. Specimens were heated quickly by an induction coil through a graphite heater and were stressed immediately after the intended temperature was reached. The inside of the high-temperature chamber was kept at a vacuum of  $10^{-5}$  Torr. Dislocations were revealed by etching the (100) surface.

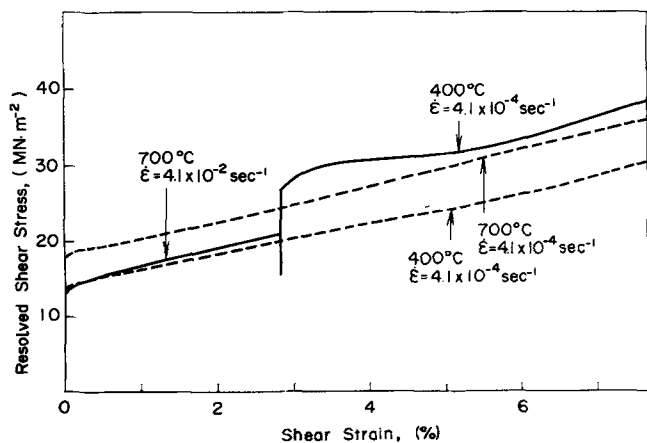


Figure 3 The stress-strain curve of specimen B deformed first at 700°C and  $\dot{\epsilon} = 4.1 \times 10^{-2} \text{ sec}^{-1}$  and subsequently at 400°C and  $\dot{\epsilon} = 4.1 \times 10^{-4} \text{ sec}^{-1}$ . Stress-strain curves for  $\dot{\epsilon} = 4.1 \times 10^{-4} \text{ sec}^{-1}$  at 400°C and for  $\dot{\epsilon} = 4.1 \times 10^{-4} \text{ sec}^{-1}$  at 700°C throughout a whole deformation stage are also shown.

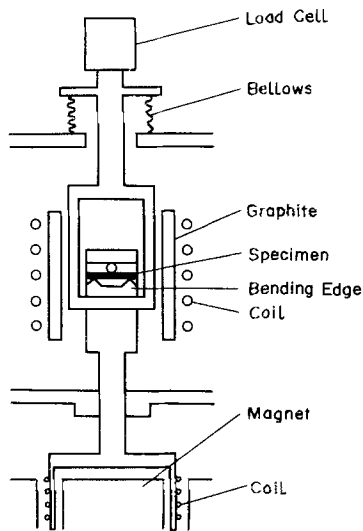


Figure 4 A schematic picture of the stressing apparatus used for the measurements of dislocation velocity.

By stressing the specimens, the movements of isolated loops were observed in the temperature range below 300° C. However, when the specimens were brought to the temperature range above 400° C, the motion of such loops due to stressing was no longer observed irrespective of their nature; edge or screw. Increase of the applied stress in such a temperature range resulted in the formation of slip bands initiating from such loops or from some other places in the specimen. This was true in all specimens. The critical temperature for the occurrence of this phenomenon was observed to depend on the time taken to heat up the specimen. Rapid heating shifted the critical temperature to the higher temperature side. It is thought that fresh dislocations introduced at room temperature become locked by impurities during heating at 300 to 400° C.

Measurements of the velocities of dislocations in the temperature range below 300° C were done by the usual double-etching method with use of isolated half loops of fresh dislocations, the stress being applied by means of four-point bending. Measurements for the temperature range above 400° C were conducted in the following way, since all the isolated loops were locked by impurities in such a temperature range. A scratch was drawn on the (1 0 0) surface in the direction of the long axis [010] of the specimen by a diamond stylus at room temperature. The specimen was then brought to the temperature for the measurements and the stress was applied by means of three-point bending.

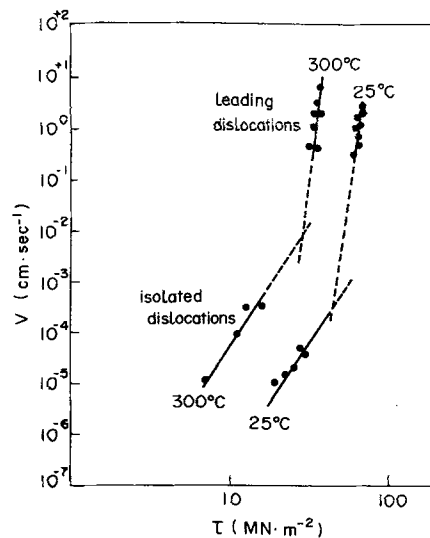


Figure 5 The velocity  $v$  versus the shear stress  $\tau$  relations for isolated screw dislocations and for leading screw dislocations of the arrays in specimen A at 25 and 300° C.

Groups of dislocation etch pits emerging from the scratch were developed by etching the surface after the stressing. The velocity of dislocations was determined by dividing the distance travelled by leading dislocations of the arrays by the duration of the stress pulse. Dislocations nucleated from such a scratch and observed on the (100) surface were mostly screw. Arrays of edge dislocations on the (100) surface were not developed from the scratch but from the edge of the specimen. This was common to all specimens. The velocity of screw dislocations was always observed to be lower than that of edge dislocations by about an order of magnitude irrespective of the kind of specimen. Thus, measurements were conducted only for screw dislocations.

It was questioned whether the dynamic characteristics were different between isolated dislocations and leading dislocations of arrays. Therefore, the comparison was made in the temperature range below 300° C.

Fig. 5 shows velocity data for isolated and leading screw dislocations for specimen A in the low temperature range. The velocity  $v$  of both kinds of dislocations can be expressed well by a following equation:

$$v = v_0 \left( \frac{\tau}{\tau_0} \right)^m \quad (1)$$

where  $v_0 = 1 \text{ cm sec}^{-1}$  and  $\tau$  is the resolved shear stress. Magnitudes of  $m$  and  $\tau_0$  are given in Table

TABLE II Magnitudes of  $m$  and  $\tau_0$  for isolated screw dislocations and for leading screw dislocations in arrays for specimen A

Temperature (°C)	$m$		$\tau_0$ (MN m <sup>-2</sup> )	
	Isolated	Leading	Isolated	Leading
-196	11.3	—	250	—
25	5.0	20	230	66
300	4.8	23	74	35

II for two kinds of dislocations. It is seen that the magnitude of  $m$  of isolated dislocations at 25 and 300°C is of the order of 5, while that of leading dislocations is of the order of 20. Dislocations were nucleated from the scratches only in a stress range which is higher than that where the velocity measurements for isolated dislocations were done. Thus, it is difficult to see whether such a disagreement in values of  $m$  is due to the effect of the interaction between many dislocations nucleated from the same scratch or due to the dependence of  $m$  on the stress. However, it is to be noted that the temperature dependence of the velocity of the two kinds of dislocation accords, at least, qualitatively with each other.

Fig. 6 shows the velocity of leading screw dis-

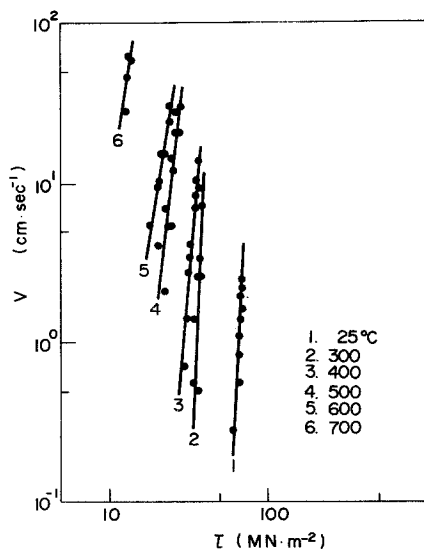


Figure 6 The velocity  $v$  of leading screw dislocations of the arrays at various temperatures plotted against the shear stress  $\tau$  in specimen A.

\*The above velocity data are found not to be described by a simple Arrhenius-type equation: the activation energy of the dislocation motion under some given stress is obtained as being different for different temperature ranges, and also the stress-dependence of the activation energy is different for different temperature ranges. However, the magnitude of the activation volume determined at each temperature range seems to be consistent with a model where the thermally activated overcoming of dispersed obstacles controls the dislocation motion.

TABLE III Magnitudes of  $m$  and  $\tau_0$  for leading screw dislocations in arrays at various temperatures. Columns A, B and C shows the data for specimens A, B and C respectively

Temperature (°C)	$m$			$\tau_0$ (MN m <sup>-2</sup> )		
	A	B	C	A	B	C
25	20	13	—	66	95	—
300	23	23	23	35	55	85
400	11	19	23	30	49	66
500	9	15	17	19	36	48
600	6	15	18	14	19	40
700	7	14	10	7.1	16	26

locations in specimen A at various temperatures, plotted against stress. For all specimens and throughout the stress and temperature ranges investigated the velocity is well expressed by Equation 1 as a function of the stress. Magnitudes of  $m$  and  $\tau_0$  at various temperatures are shown in Table III. In all specimens,  $\tau_0$  decreases monotonically with the increase in temperature. At each temperature the magnitude of  $\tau_0$  is the highest in specimen C and the lowest in specimen A. The magnitude of  $m$  is lower in specimen A than in specimens B and C in the temperature range above 400°C, while those of specimen B and C are almost the same. It is thus concluded that the dislocation velocity decreases as the concentration of trivalent impurities increases and the temperature decreases. It is interesting to note that the mobility of dislocations increases rapidly with temperature even in the temperature range where CRSS increases with the temperature. It may be suggested that the motion of screw dislocations in the temperature range 20 to 700°C and the velocity range 10<sup>-1</sup> to 10 cm sec<sup>-1</sup> is controlled by the thermally activated overcoming of obstacles associated with trivalent impurities.\*

## 5. Indentation experiments

The stress range where velocities of dislocations were measured in Section 4 lies somewhat higher than the level of CRSS measured in Section 3 at each temperature. Dislocations were not able to be generated from scratches under stresses below the range where the measurements in Table III were done. Thus, it was thought possible that the mobility of dislocations would show some peculiar

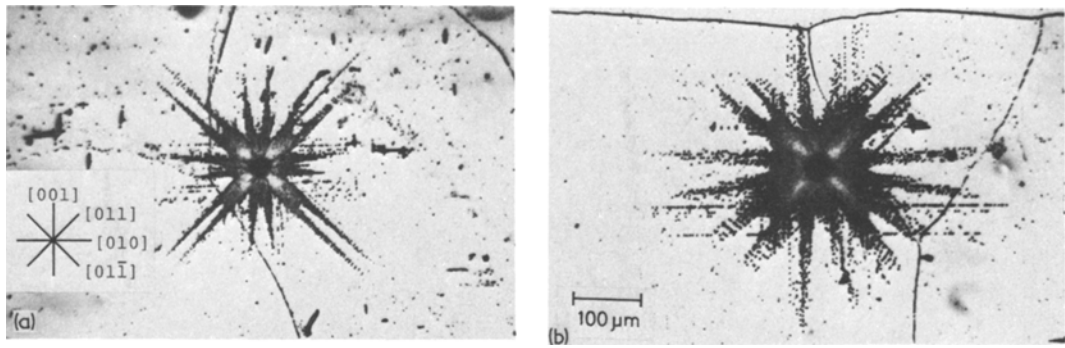


Figure 7 Rosette patterns of dislocation etch pits developed around the indentations made under a load of 1 MN on the (1 0 0) surface of specimen B at (a) 300°C, and (b) 600°C.

behaviour in the temperature dependence at the stress level of CRSS. To see the kinetic behaviour of dislocations in such a low stress level, indentations were made on the (1 0 0) surface of specimen B at various temperatures in an argon gas atmosphere and the spread of a rosette pattern of dislocation etch pits developed around indentations was measured as a function of temperature. A Nikon High-Temperature Microhardness Tester with a diamond pyramidal indenter was used.

Fig. 7a and b show the rosette patterns developed around indentations made at 300 and 600°C, respectively. It can readily be seen that arrays of etch pits developed along  $\langle 0 1 1 \rangle$  directions show edge dislocation arrays and those developed along  $\langle 0 1 0 \rangle$  screw dislocation arrays. Thus, a group of arrays along  $\langle 0 1 1 \rangle$  are called a wing of edge dislocations and that along  $\langle 0 1 0 \rangle$  a wing of screw dislocations. The main part of a wing of edge dislocations developed at 300°C consists of two parallel arrays. The spread in the width of the wing developed at 600°C is remarkable, as seen from Fig. 7b. Arrays in the same wing of screw dislocations are not necessarily parallel to each other irrespective of the temperature at which they were formed. This seems to show that screw dislocations undergo cross-slip during the development of the wing. Spread of the width of wings by increase in temperature is more remarkable in wings of edge dislocations than in those of screw dislocation. This suggests that climb of edge dislocations takes place at elevated temperatures.

It is interesting to note in Fig. 7 that the length of the wings of edge dislocations is larger than that of screw dislocation in the rosette developed at 300°C, while the reverse holds in the rosette developed at 600°C. Fig. 8 shows the lengths of the

wings of edge and screw dislocations for an indentation load of 1 MN plotted against the temperature where the rosette developed. The length of the wings of edge dislocations increases with increase in temperature up to 200°C. It shows a maximum at around 200°C, and then decreases with increasing temperature. This decrease in the length is related to the spread in the width. On the other hand, the length of the wings of screw dislocations increases linearly with temperature. Thus, although the wings of edge dislocations are larger than those of screw dislocations at low temperatures, the situation is reversed in the temperature range above 400°C.

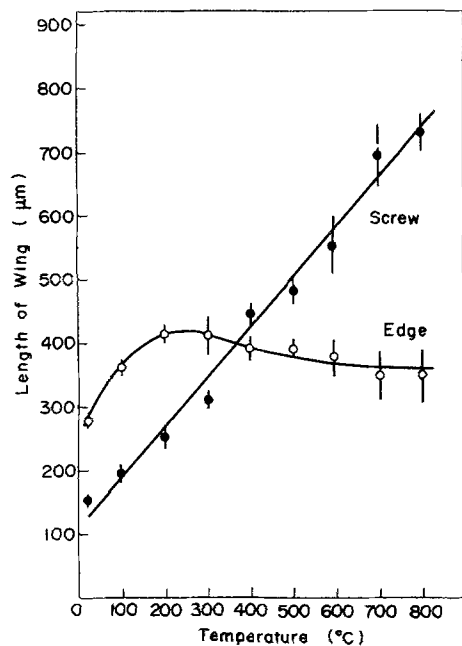


Figure 8 The lengths of the wings developed under a load of 1 MN in specimen B plotted against indentation temperature. Open marks are for the edge wings and solid marks for the screw wings.

The force acting on each dislocation is thought to be a decreasing function of the distance from the indentation. The velocity of dislocations therefore decreases with the distance travelled. The result in Fig. 8 may be interpreted as that some effect, which interrupts the slow motion of only edge dislocations, operates at temperatures around 200° C, becoming dominant as the temperature increases. Possibly, this would be the trapping of slowly moving edge dislocations by the formation of Cottrell atmosphere due to the increased mobility of impurities.

## 6. *In situ* observations of dislocations under stress at elevated temperature

The dynamic behaviour of dislocations in the specimens under applied stress at elevated temperatures was observed by transmission electron microscopy with use of high-voltage electron microscope JEM 1000 equipped with a high-temperature tensile stage. Observations were made at an accelerating voltage of 1000 kV and the behaviour of dislocations was recorded by a VTR. Specimens for *in situ* observations were prepared from cleaved specimens with a shape of a thin plate  $3 \times 8 \times 0.5$  mm<sup>3</sup> in size. They were thinned mechanically to 0.3 mm thickness and then subjected to a jet polishing.

Throughout the temperature range between room temperature and 700° C screw dislocations were observed to move much slower than edge and mixed-type dislocations. The velocities of both edge and screw dislocations increased rapidly with increase in temperature.

At room temperature, dislocations of both screw and edge orientations were observed to move smoothly and slowly and no jerky motion was observed. Dislocations in edge orientation were

relatively straight while those of screw orientation contained cusps. These characteristics in the shape agreed with the observations by Appel *et al.* [11, 12].

At temperatures higher than 400° C, fresh dislocations introduced at room temperature were all observed to be locked. Their motion was not observed even when the stress was increased, irrespective of the type of dislocation. The motion of dislocation of both edge and screw orientations in the temperature range 500 to 700° C was observed to be no longer smooth but extremely jerky. Screw dislocations contained many dragging points along them. Under stress, loops first bowed out around such dragging points and then a whole dislocation moved. Dislocations of screw orientation containing cusps due to such dragging points are shown in Fig. 9.

## 7. Discussion

The temperature dependence of CRSS of MgO crystals observed in the present investigation is like that observed in fcc alloy crystals. However, a remarkable difference between these two materials is also observed. Namely, while the plateau in alloy crystals is usually characterized by the insensitivity to the strain rate, the appearance of the plateau in MgO crystals is largely influenced by strain rate.

The plateau in MgO crystals seems to appear as a result of the balance of the general tendency of the decrease in CRSS due to the increase in temperature and the anomalous increase of CRSS in the intermediate temperature range.

The mobility of screw dislocations measured by the etch-pit method is lower than that of edge dislocations throughout the temperature range 25 to 700° C and is observed to decrease with increase in concentration of all kinds of impurity and also

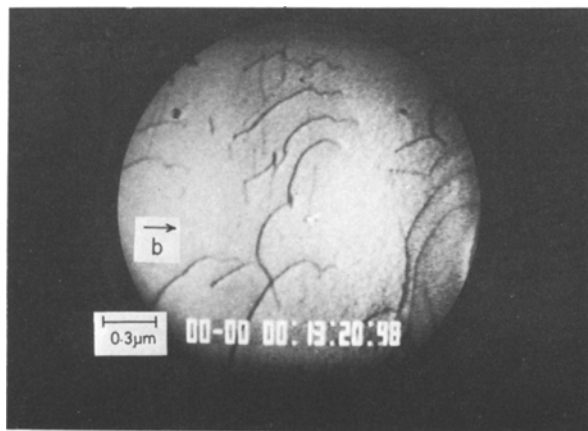


Figure 9 Moving dislocations of screw orientation with accompanying dragging points observed by *in situ* deformation at 700° C in a high-voltage electron microscope.



that of trivalent impurities. Such dynamic characteristics of screw dislocations may be related to a general tendency for decrease in CRSS with increase in the temperature. However, the appearance of the maximum in CRSS at elevated temperatures can never be interpreted from such behaviour of screw dislocations.

It has been observed by the etch-pit method and also by *in situ* observations by HVEM, that fresh dislocations introduced at room temperature become locked when the crystal is brought to 300 to 400° C. In Section 5 it was shown that edge dislocations are trapped and locked at temperatures above 200 to 300° C when they are moving at low velocities. These temperatures are close to the temperature where the plateau begins. If we adopt the view point that the plateau appears as a result of the balance of two phenomena having opposing temperature dependence of the CRSS as mentioned before, the maximum of CRSS may be interpreted to be related to such locking of dislocations occurring at elevated temperatures. It should be emphasized, however, that the origin of the maximum in specimen A seems to be different from that in specimen B since the dependence of the maximum temperature on the strain rate is different between these specimens.

The origin of the maximum in specimen B is now discussed. The characteristic in the motion of dislocations in specimen B at temperatures above 500° C observed by HVEM is the jerkiness, while the motion is smooth at lower temperatures. Such jerky motion would possibly be related to the increase in CRSS with temperature.

The magnitude of the velocity of screw dislocations at 700° C as obtained by substituting the magnitude of CRSS for  $\dot{\epsilon} = 4.1 \times 10^{-4} \text{ sec}^{-1}$  into the mobility data in Section 4 seems to be too high to explain the strain rate of the specimens since the density of mobile dislocations is thought to be of order of  $10^6$  or  $10^7 \text{ cm}^{-2}$  from etch pit observations. Thus, it may be reasonable to think that dislocations overcome local obstacles such as clusters of impurity atoms and other dislocations by the thermal activation during macroscopic deformation. Each dislocation has to spend some waiting time at these obstacles.

An atmosphere of impurity atoms would naturally be developed around the dislocations during such a waiting period since the diffusion rate of impurities is rather high at the temperatures concerned. Thus, in addition to the resistance

due to the original obstacles, the dislocations have to overcome the resistance due to such an atmosphere when they start again and contribute to the deformation. This would result in a remarkably jerky nature of dislocation motion as is observed by HVEM. In the case where the density of mobile dislocations is rather insensitive to strain rate, the average velocity of dislocations and, therefore, the waiting period, are controlled by the strain rate. A higher strain rate corresponds to a shorter waiting period and, in turn, a lower resistance due to the atmosphere since the atmosphere is not fully developed within a shorter waiting period. The reverse holds for a lower strain rate. This explains well the anomalous strain rate dependence of CRSS in specimen B observed at 700° C.

As the temperature is raised, the diffusion rate of impurity atoms increases and the formation of the atmosphere is enhanced, resulting in the increase in CRSS for the deformation at a constant strain rate, as long as the density of mobile dislocations is insensitive to the temperature. With further increase in temperature, the release of dislocations from the atmosphere will also be enhanced by the thermal activation. Thus, a maximum in CRSS results at a certain temperature.

As the strain rate is increased, the temperature for the maximum shifts to the high temperature side, since the waiting period becomes shorter and the release rate of dislocations from the atmosphere is increased. This is consistent with the results seen in Fig. 1a and b.

For the same atmosphere formed around dislocations, a higher stress is needed at lower temperature to release dislocations at a given rate. Thus, the CRSS of specimens having an atmosphere developed during deformation at 700° C should be measured as being higher at 400° C than at 700° C for the deformation at the same strain rate. This gives an explanation for the facts shown in Figs. 2 and 3. The atmosphere developed during deformation at 400° C is weaker than that developed at 700° C. Such a situation may be responsible for the fact that the slope of the stress-strain curve at 400° C of a specimen previously deformed at 700° C is low, or even negative, in the deformation stage after the yielding.

It has been observed in Section 5 that edge dislocations are more effectively retarded by impurities than screw dislocations, at elevated temperatures. Furthermore, the behaviour of CRSS against temperature is observed to be similar be-

tween specimens B and C, except at 800° C. These facts suggest that the important impurities for the anomalous behaviour of CRSS are not trivalent but Ca<sup>2+</sup>. As an impurity, Ca<sup>2+</sup> can interact strongly with edge dislocations since its ionic radius is 0.99 Å, being much larger than that of Mg<sup>2+</sup> (0.65 Å).

The origin for the peak at 700° C observed in specimen A is not understood at present. It seems to be of an athermal nature since the peak temperature is not shifted by change in strain rate. However, there is no plausible explanation for the absence of this type of peak in specimens B and C deformed at high strain rates. It is to be noted that the temperature dependence of CRSS in specimens B and C in the temperature range 300 to 700° C is somewhat irregular. Some additional processes which affect the magnitude of CRSS may be operative in this temperature range.

### Acknowledgement

Chambers and jigs for high-temperature experiments were produced by the members of the machine shop of the Research Institute for Iron, Steel and Other Metals to which the authors wish to express their gratitude.

### References

1. M. SRINIVASAN and T. G. STOEBE, *J. Appl. Phys.* **41** (1970) 3726.
2. *Idem*, *J. Mater. Sci.* **8** (1973) 1567.
3. *Idem*, *ibid* **9** (1974) 121.
4. B. REPPICH, *Acta Met.* **20** (1972) 557.
5. *Idem*, *Mat. Sci. Eng.* **19** (1975) 51.
6. M. N. SINHA, D. J. LLOYD and K. TANGRI, *Phil. Mag.* **28** (1973) 1341.
7. R. N. SINGH and P. L. COBLE, *J. Appl. Phys.* **45** (1974) 981.
8. *Idem*, *ibid* **45** (1974) 990.
9. *Idem*, *ibid* **45** (1974) 5129.
10. S. N. VALKOVSKII and E. M. NADGORNYYI, *Sov. Phys. Solid State* **17** (1976) 1733.
11. F. APPEL, H. BETHGE and U. MESSERSCHMIDT, *Phys. Stat. Sol. (a)* **38** (1976) 103.
12. *Idem*, *ibid* **42** (1977) 61.
13. R. W. DAVIDGE, *J. Mater. Sci.* **2** (1967) 339.
14. S. M. COPLEY and B. H. KEAR, *Trans. Met. Soc.* **239** (1967) 977.
15. P. H. THORNTON, R. G. DAVIES and T. L. JOHNSTON, *Met. Trans* **1** (1970) 207.
16. S. TAKEUCHI and E. KURAMOTO, *Acta Met.* **21** (1973) 415.

Received 7 August and accepted 27 November 1979.